

HySST: A Stable Sparse Rapidly-Exploring Random Trees Optimal Motion Planning Algorithm for Hybrid Dynamical Systems*

Nan Wang and Ricardo G. Sanfelice

Abstract—This paper proposes a stable sparse rapidly-exploring random trees (SST) algorithm to solve the optimal motion planning problem for hybrid systems. At each iteration, the proposed algorithm, called HySST, selects a vertex with the lowest cost among all the vertices within the neighborhood of a randomly selected sample and then extends the search tree by flow or jump, which is also chosen randomly when both regimes are possible. In addition, HySST maintains a static set of witness points such that all the vertices within the neighborhood of each witness are pruned except the vertex with the lowest cost. Through a definition of concatenation of functions defined on hybrid time domains, we show that HySST is asymptotically near optimal, namely, the probability of failing to find a motion plan such that its cost is close to the optimal cost approaches zero as the number of iterations of the algorithm increases to infinity. This property is guaranteed under mild conditions on the data defining the motion plan, which include a relaxation of the usual positive clearance assumption imposed in the literature of classical systems. The proposed algorithm is applied to an actuated bouncing ball system and a collision-resilient tensegrity multicopter system so as to highlight its generality and computational features.

I. INTRODUCTION

Motion planning consists of finding a state trajectory and associated inputs that connect the initial and final state sets while satisfying the dynamics of the systems and given safety requirements. Motion planning for purely continuous-time systems and purely discrete-time systems has been well studied in the literature; see e.g., [1]. In recent years, several (feasible) motion planning algorithms have been developed, including graph search algorithms [2], artificial potential field methods [3] and sampling-based algorithms. The sampling-based algorithms have drawn much attention in recent years because of their fast exploration speed for high dimensional problems and theoretical guarantees; specially, probabilistic completeness, which means that the probability of failing to find a motion plan converges to zero, as the number of samples approaches infinity. Two popular sampling-based algorithms are the probabilistic roadmap (PRM) algorithm [4] and the rapidly-exploring random tree (RRT) algorithm [5]. The PRM method relies on the existence of a steering function returning the solution of a two-point boundary value problem (TPBVP). Unfortunately, solutions to TPBVPs are difficult to generate for most dynamical systems. On the other

hand, RRT algorithm does not require a steering function. Arguably, RRT is perhaps the most successful algorithm to solve feasible motion planning problems.

A feasible solution is not sufficient in most applications as the quality of the solution returned by the motion planning algorithms is key [6]. It has been shown in [7] that the solution returned by RRT converges to a sub-optimal solution. Therefore, variants of PRM and RRT, such as PRM* and RRT* [8], have been developed to solve optimal motion planning problems with guaranteed asymptotic optimality. However, both PRM* and RRT* require a steering function, which prevents them from being widely applied. On the other hand, the stable sparse RRT (SST) algorithm [9] does not require a steering function and is guaranteed to be asymptotically near optimal, which means that the probability of finding a solution that has a cost close to the minimal cost converges to one as the number of iterations goes to infinity.

The aforementioned motion planning algorithms have been widely applied to purely continuous-time and purely discrete-time systems. However, much less efforts have been devoted to the motion planning for hybrid systems. In our previous work [10], a feasible motion planning problem is formulated for hybrid system given in terms of hybrid equations as in [11], which is a general framework that captures a broad class of hybrid systems. In [10], the hybrid RRT algorithm is designed to solve the feasible motion planning problem for such systems with guaranteed probabilistic completeness. In this paper, we propose a motion planning algorithm for hybrid systems with the goal of assuring (asymptotic) optimality of the solution. We formulate the optimal motion planning problem for hybrid systems inspired by the feasible motion planning problems in [10]. Then, we design an SST-type algorithm to solve the optimal motion planning problem for hybrid systems. Following [9], the proposed algorithm, called HySST, incrementally constructs a search tree rooted in the initial state set toward the random samples. At first, HySST draws samples from the state space. Then, it selects a vertex such that the state associated with this vertex is within a ball centered at the random sample and has minimal cost. Next, HySST propagates the state trajectory from the state associated with the selected vertex, and adds a new vertex and edge from the propagated trajectory. In addition, HySST maintains a static set of state points, called witnesses, to represent the explored regions in the state space. HySST also employs a pruning process to guarantee that only a single vertex with lowest cost is kept within the neighborhood of each witness. We show that, under mild assumptions, HySST is asymptotically near-optimal. To the

*Research partially supported by NSF Grants no. ECS-1710621, CNS-2039054, and CNS-2111688, by AFOSR Grants no. FA9550-19-1-0053, FA9550-19-1-0169, and FA9550-20-1-0238, and by ARO Grant no. W911NF-20-1-0253.

Nan Wang and Ricardo G. Sanfelice are with the Department of Electrical and Computer Engineering, University of California, Santa Cruz, CA 95064, USA; nanwang@ucsc.edu, ricardo@ucsc.edu

authors' best knowledge, it is the first optimal RRT-type algorithm for systems with hybrid dynamics. The proposed algorithm is illustrated in an actuated bouncing ball system and a collision-resilient tensegrity multicopter system.

The remainder of the paper is structured as follows. Section II presents notation and preliminaries. Section III presents the problem statement and introduction of applications. Section IV presents the HySST algorithm. Section V presents the analysis of the asymptotic near optimality of HySST algorithm. Section VI presents the illustration of HySST in the examples. Proofs and more details are given [12].

II. NOTATION AND PRELIMINARIES

A. Notation

The real numbers are denoted as \mathbb{R} and its nonnegative subset is denoted as $\mathbb{R}_{\geq 0}$. The set of nonnegative integers is denoted as \mathbb{N} . The notation $\text{int } S$ denotes the interior of the set S . The notation \overline{S} denotes the closure of the set S . The notation ∂S denotes the boundary of the set S . The notation $\text{rge } f$ denotes the range of the function f . The notation \mathbb{B} denotes the closed unit ball of appropriate dimension in the Euclidean norm. The notation $c + r\mathbb{B}$ denotes the closed ball of appropriate dimension in the Euclidean norm centered at c with radius r . Given sets $P \subset \mathbb{R}^n$ and $Q \subset \mathbb{R}^n$, the Minkowski sum of P and Q , denoted as $P + Q$, is the set $\{p + q : p \in P, q \in Q\}$.

B. Preliminaries

A hybrid system \mathcal{H} with inputs is modeled as [13]

$$\mathcal{H} : \begin{cases} \dot{x} = f(x, u) & (x, u) \in C \\ x^+ = g(x, u) & (x, u) \in D \end{cases} \quad (1)$$

where $x \in \mathbb{R}^n$ is the state, $u \in \mathbb{R}^m$ is the input, $C \subset \mathbb{R}^n \times \mathbb{R}^m$ represents the flow set, $f : \mathbb{R}^n \times \mathbb{R}^m \rightarrow \mathbb{R}^n$ represents the flow map, $D \subset \mathbb{R}^n \times \mathbb{R}^m$ represents the jump set, and $g : \mathbb{R}^n \times \mathbb{R}^m \rightarrow \mathbb{R}^n$ represents the jump map, respectively. The continuous evolution of x is captured by the flow map f . The discrete evolution of x is captured by the jump map g . The flow set C collects the points where the state can evolve continuously. The jump set D collects the points where jumps can occur.

Given a flow set C , the set $U_C := \{u \in \mathbb{R}^m : \exists x \in \mathbb{R}^n \text{ such that } (x, u) \in C\}$ includes all possible input values that can be applied during flows. Similarly, given a jump set D , the set $U_D := \{u \in \mathbb{R}^m : \exists x \in \mathbb{R}^n \text{ such that } (x, u) \in D\}$ includes all possible input values that can be applied at jumps. These sets satisfy $C \subset \mathbb{R}^n \times U_C$ and $D \subset \mathbb{R}^n \times U_D$. Given a set $K \subset \mathbb{R}^n \times U_*$, where $*$ is either C or D , we define $\Pi_*(K) := \{x : \exists u \in U_* \text{ s.t. } (x, u) \in K\}$ as the projection of K onto \mathbb{R}^n , and define $C' := \Pi_C(C)$ and $D' := \Pi_D(D)$.

In addition to ordinary time $t \in \mathbb{R}_{\geq 0}$, we employ $j \in \mathbb{N}$ to denote the number of jumps of the evolution of x and u for \mathcal{H} in (1), leading to hybrid time (t, j) for the parameterization of its solutions and inputs. The domain

of a solution to \mathcal{H} is given by a hybrid time domain. A hybrid time domain is defined as a subset E of $\mathbb{R}_{\geq 0} \times \mathbb{N}$ that, for each $(T, J) \in E$, $E \cap ([0, T] \times \{0, 1, \dots, J\})$ can be written as $\cup_{j=0}^J ([t_j, t_{j+1}], j)$ for some finite sequence of times $0 = t_0 \leq t_1 \leq t_2 \leq \dots \leq t_{J+1} = T$. A hybrid arc $\phi : \text{dom } \phi \rightarrow \mathbb{R}^n$ is a function on a hybrid time domain that, for each $j \in \mathbb{N}$, $t \mapsto \phi(t, j)$ is locally absolutely continuous on each interval $I^j := \{t : (t, j) \in \text{dom } \phi\}$ with nonempty interior. The definition of solution pair to a hybrid system is given as follows. For more details, see [11].

Definition 2.1 (Solution pair to a hybrid system):

Given a pair of functions $\phi : \text{dom } \phi \rightarrow \mathbb{R}^n$ and $u : \text{dom } u \rightarrow \mathbb{R}^m$, (ϕ, u) is a solution pair to (1) if $\text{dom}(\phi, u) := \text{dom } \phi = \text{dom } u$ is a hybrid time domain, $(\phi(0, 0), u(0, 0)) \in \overline{C} \cup D$, and the following hold:

- 1) For all $j \in \mathbb{N}$ such that I^j has nonempty interior,
 - a) the function $t \mapsto \phi(t, j)$ is locally absolutely continuous,
 - b) $(\phi(t, j), u(t, j)) \in C$ for all $t \in \text{int } I^j$,
 - c) the function $t \mapsto u(t, j)$ is Lebesgue measurable and locally bounded,
 - d) for almost all $t \in I^j$, $\dot{\phi}(t, j) = f(\phi(t, j), u(t, j))$.
- 2) For all $(t, j) \in \text{dom}(\phi, u)$ such that $(t, j + 1) \in \text{dom}(\phi, u)$,

$$(\phi(t, j), u(t, j)) \in D \quad \phi(t, j + 1) = g(\phi(t, j), u(t, j)).$$

HySST requires concatenating solution pairs. The concatenation operation of solution pairs is defined next.

Definition 2.2: (Concatenation operation) Given two functions $\phi_1 : \text{dom } \phi_1 \rightarrow \mathbb{R}^n$ and $\phi_2 : \text{dom } \phi_2 \rightarrow \mathbb{R}^n$, where $\text{dom } \phi_1$ and $\text{dom } \phi_2$ are hybrid time domains, ϕ_2 can be concatenated to ϕ_1 if ϕ_1 is compact and $\phi : \text{dom } \phi \rightarrow \mathbb{R}^n$ is the concatenation of ϕ_2 to ϕ_1 , denoted $\phi = \phi_1 | \phi_2$, namely,

- 1) $\text{dom } \phi = \text{dom } \phi_1 \cup (\text{dom } \phi_2 + \{(T, J)\})$, where $(T, J) = \max \text{dom } \phi_1$ and the plus sign denotes Minkowski addition;
- 2) $\phi(t, j) = \phi_1(t, j)$ for all $(t, j) \in \text{dom } \phi_1 \setminus \{(T, J)\}$ and $\phi(t, j) = \phi_2(t - T, j - J)$ for all $(t, j) \in \text{dom } \phi_2 + \{(T, J)\}$.

III. PROBLEM STATEMENT

The feasible motion planning problem for hybrid systems is defined in [10] as follows.

Problem 1: (Feasible motion planning) Given a hybrid system \mathcal{H} with input $u \in \mathbb{R}^m$ and state $x \in \mathbb{R}^n$, the initial state set $X_0 \subset \mathbb{R}^n$, the final state set $X_f \subset \mathbb{R}^n$, and the unsafe set $X_u \subset \mathbb{R}^n \times \mathbb{R}^m$, find a pair $(\phi, u) : \text{dom}(\phi, u) \rightarrow \mathbb{R}^n \times \mathbb{R}^m$, namely, a *motion plan*, such that for some $(T, J) \in \text{dom}(\phi, u)$, the following hold:

- 1) $\phi(0, 0) \in X_0$, namely, the initial state of the solution belongs to the given initial state set X_0 ;
- 2) (ϕ, u) is a solution pair to \mathcal{H} as defined in Definition 2.1;
- 3) (T, J) is such that $\phi(T, J) \in X_f$, namely, the solution belongs to the final state set at hybrid time (T, J) ;

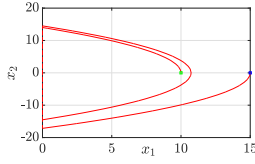


Fig. 1. A motion plan to the sample motion planning problem for actuated bouncing ball system.

- 4) $(\phi(t, j), u(t, j)) \notin X_u$ for each $(t, j) \in \text{dom}(\phi, u)$ such that $t + j \leq T + J$, namely, the solution pair does not intersect with the unsafe set before its state trajectory reaches the final state set.

Therefore, given sets X_0, X_f and X_u , and a hybrid system \mathcal{H} with data (C, f, D, g) , a (feasible) motion planning problem \mathcal{P} is formulated as $\mathcal{P} = (X_0, X_f, X_u, (C, f, D, g))$.

Let Σ denote the set of all solution pairs to \mathcal{H} . Let Σ_ϕ denote the set of state trajectories of all the solution pairs in Σ . The optimal motion planning problem for hybrid systems consists of finding a feasible motion plan with minimum cost [8, Problem 3].

Problem 2: (Optimal motion planning) Given a motion planning problem $\mathcal{P} = (X_0, X_f, X_u, (C, f, D, g))$ and a cost functional $c : \Sigma_\phi \rightarrow \mathbb{R}_{\geq 0}$ where $\Sigma := \{(\phi, u) : (\phi, u) \text{ is a solution pair to } (C, f, D, g)\}$ and $\Sigma_\phi := \{\phi : \exists u : \text{dom } \phi \rightarrow \mathbb{R}^m \text{ such that } (\phi, u) \in \Sigma\}$, find a feasible motion plan (ϕ^*, u^*) to Problem 1 such that $(\phi^*, u^*) = \arg \min_{(\phi, u) \in \Sigma} c(\phi)$. Given sets X_0, X_f and X_u , a hybrid system \mathcal{H} with data (C, f, D, g) , and a cost functional c , an optimal motion planning problem \mathcal{P}^* is formulated as $\mathcal{P}^* = (X_0, X_f, X_u, (C, f, D, g), c)$.

Problem 2 is illustrated in the following examples.

Example 3.1: (Actuated bouncing ball system) Consider a ball bouncing on a fixed horizontal surface. The surface is located at the origin and, through control actions, is capable of affecting the velocity of the ball after the impact. The dynamics of the ball while in the air is given by $\dot{x} = \begin{bmatrix} x_2 \\ -\gamma \end{bmatrix} =: f(x, u), (x, u) \in C$ where $x := (x_1, x_2) \in \mathbb{R}^2$. The height of the ball is denoted by x_1 . The velocity of the ball is denoted by x_2 . The gravity constant is denoted by γ . The flow is allowed when the ball is above the surface. Hence, the flow set is $C := \{(x, u) \in \mathbb{R}^2 \times \mathbb{R} : x_1 \geq 0\}$. At every impact, the velocity of the ball changes from pointing down to pointing up while the height remains the same. The dynamics at jumps of the actuated bouncing ball system is given as $x^+ = \begin{bmatrix} x_1 \\ -\lambda x_2 + u \end{bmatrix} =: g(x, u), (x, u) \in D$ where $u \geq 0$ is the input and $\lambda \in (0, 1)$ is the coefficient of restitution. The jump is allowed when the ball is on the surface with negative velocity. Hence, the jump set is $D := \{(x, u) \in \mathbb{R}^2 \times \mathbb{R} : x_1 = 0, x_2 \leq 0, u \geq 0\}$.

Given the initial state set $X_0 = \{(15, 0)\}$, the final state set $X_f = \{(10, 0)\}$, and the unsafe set $X_u = \{(x, u) \in \mathbb{R}^2 \times \mathbb{R} : x_1 \in [20, \infty), u \in [5, \infty)\}$, an instance of the optimal motion planning problem for the actuated bouncing ball system is to

find a motion plan that has minimal hybrid time. To capture the hybrid time domain information, an auxiliary state $\tau \in \mathbb{R}_{\geq 0}$ representing the normal time and an auxiliary state $k \in \mathbb{N}$ representing the jump numbers are imported. An auxiliary hybrid system $\bar{\mathcal{H}} := (\bar{C}, \bar{f}, \bar{D}, \bar{g})$ with state $\bar{x} := (x, \tau, k) \in \mathbb{R}^2 \times \mathbb{R}_{\geq 0} \times \mathbb{N}$ is constructed as follows

- 1) $\bar{C} := \{(\bar{x}, u) \in \mathbb{R}^2 \times \mathbb{R}_{\geq 0} \times \mathbb{N} \times \mathbb{R} : (x, u) \in C\}$;
- 2) $\bar{f}(\bar{x}, u) := \begin{bmatrix} f(x, u) \\ 1 \\ 0 \end{bmatrix}, (\bar{x}, u) \in \bar{C}$;
- 3) $\bar{D} := \{(\bar{x}, u) \in \mathbb{R}^2 \times \mathbb{R}_{\geq 0} \times \mathbb{N} \times \mathbb{R} : (x, u) \in D\}$;
- 4) $\bar{g}(\bar{x}, u) := \begin{bmatrix} g(x, u) \\ \tau \\ k + 1 \end{bmatrix}, (\bar{x}, u) \in \bar{D}$.

with the X_0, X_f , and X_u extended to

- 1) $\bar{X}_0 := X_0 \times (0, 0)$;
- 2) $\bar{X}_f := X_f \times \mathbb{R}_{\geq 0} \times \mathbb{N}$;
- 3) $\bar{X}_u := X_u \times \mathbb{R}_{\geq 0} \times \mathbb{N}$.

Then the cost functional c can be defined as

$$c(\bar{\phi}) = c(\phi, \tau, k) := \tau(T, J) + k(T, J) \quad (2)$$

where $\bar{\phi} = (\phi, \tau, k)$ denotes a state trajectory of the solution pair to $\bar{\mathcal{H}}$, and $(T, J) = \max \text{dom } \bar{\phi}$. Then the example optimal motion planning problem for the bouncing ball is defined as $\mathcal{P}^* = (\bar{X}_0, \bar{X}_f, \bar{X}_u, (\bar{C}, \bar{f}, \bar{D}, \bar{g}), c)$

Example 3.2: (Collision-resilient tensegrity multicopter system [14]) Consider a collision-resilient tensegrity multicopter in horizontal plane that can operate after colliding with a concrete wall. The state of the multicopter is composed of the position vector $p := (p_x, p_y) \in \mathbb{R}^2$, where p_x denotes the position along x -axis and p_y denotes the position along y -axis, the velocity vector $v := (v_x, v_y) \in \mathbb{R}^2$, where v_x denotes the velocity along x -axis and v_y denotes the velocity along y -axis, and the acceleration vector $a := (a_x, a_y) \in \mathbb{R}^2$ where a_x denotes the acceleration along x -axis and a_y denotes the acceleration along y -axis. The state of the system is $x := (p, v, a) \in \mathbb{R}^6$ and its input is $u := (u_x, u_y) \in \mathbb{R}^2$.

The environment is assumed to be known. Define the region of the walls as $\mathcal{W} \subset \mathbb{R}^2$, represented by blue rectangles in Figure 3. Flow is allowed when the multicopter is in the free space. Hence, the flow set is $C := \{(p, v, a), u \in \mathbb{R}^6 \times \mathbb{R}^2 : p \notin \mathcal{W}\}$. The dynamics of the quadrotors when no collision occurs can be captured using time-parameterized polynomial trajectories because of its differential flatness as

$$\dot{x} = \begin{bmatrix} v \\ a \\ u \end{bmatrix} =: f(x, u), (x, u) \in C; \text{ see [15].}$$

Note that the post-collision position stays the same as the pre-collision position. Therefore, $p^+ = p$. Denote the velocity component of $v = (v_x, v_y)$ that is normal to the wall as v_n and the velocity component that is tangential to the wall as v_t . Then, the velocity component v_n after the jump is modeled as $v_n^+ = -e v_n =: g_n^v(v)$ where $e \in (0, 1)$ is the coefficient of restitution. The velocity component v_t after the jump is modeled as $v_t^+ = v_t + \kappa(-e - 1) \arctan \frac{v_t}{v_n} =: g_t^v(v)$ where $\kappa \in \mathbb{R}$ is a constant; see

[14]. Denote the projection of the updated vector (v_n^+, v_t^+) onto x axle as $\Pi_x(v_n^+, v_t^+)$ and the projection of the updated vector (v_n^+, v_t^+) onto y axle as $\Pi_y(v_n^+, v_t^+)$. Therefore,

$$v^+ = \begin{bmatrix} \Pi_x(g_n^v(v), g_t^v(v)) \\ \Pi_y(g_n^v(v), g_t^v(v)) \end{bmatrix} =: g^v(v).$$

We assume that $a^+ = 0$, which corresponds to a hovering status. The discrete dynamics capturing the collision process is modeled as $x^+ = \begin{bmatrix} p \\ g^v(v) \\ 0 \end{bmatrix} =: g(x, u), (x, u) \in D$. The jump is allowed when the multicopter is on the wall surface with positive velocity towards the wall. Hence, the jump set is $D := \{(p, v, a), u) \in \mathbb{R}^6 \times \mathbb{R}^2 : p \in \partial\mathcal{W}, v_n < 0\}$.

Given the initial state set as $X_0 = \{(1, 2, 0, 0, 0, 0)\}$, the final state set as $X_f = \{(5, 4)\} \times \mathbb{R}^4$, and the unsafe set as $X_u = \{(x, u) \in \mathbb{R}^6 \times \mathbb{R}^2 : p_x \in (\infty, 0] \cup [6, \infty), p_y \in (\infty, 0] \cup [5, \infty), (p_x, p_y) \in \text{int } \mathcal{W}\}$, an instance of the optimal motion planning problem for the collision-resilient tensegrity multicopter system is to find the motion plan with minimal hybrid time as Example 3.1.

IV. HYSST: AN OPTIMAL MOTION PLANNING ALGORITHM FOR HYBRID SYSTEMS

A. Overview

In this paper, we propose an SST algorithm for hybrid systems, which we refer to as HySST algorithm. HySST algorithm searches for the optimal motion plan by incrementally constructing a search tree. The search tree is modeled by a directed tree. A directed tree is a pair $\mathcal{T} = (V, E)$, where V is a set whose elements are called vertices and E is a set of paired vertices whose elements are called edges. The edges in a directed tree are directed, which means the pairs of vertices that represent edges are ordered. The set of edges E is defined as $E \subset \{(v_1, v_2) : v_1 \in V, v_2 \in V, v_1 \neq v_2\}$. The edge $e = (v_1, v_2) \in E$ represents an edge from v_1 to v_2 . A path in \mathcal{T} is a sequence of vertices $p = (v_1, v_2, \dots, v_k)$ such that $(v_i, v_{i+1}) \in E$ for all $i \in \{1, 2, \dots, k-1\}$. If there exists a path from the vertex v_0 to the vertex v_1 in the search tree, then v_0 is called a *parent vertex* of v_1 and v_1 is called a *child vertex* of v_0 .

Each vertex in the search tree is associated with a state value of \mathcal{H} and a cost value that estimates the cost from the root vertex up to the vertex. Each edge in the search tree is associated with a solution pair to \mathcal{H} that connects the state values associated with their endpoint vertices. The state value and the cost value associated with vertex $v \in V$ is denoted as \bar{x}_v and \bar{c}_v , respectively. The solution pair associated with edge $e \in E$ is denoted as $\bar{\psi}_e$. The solution pair that the path $p = (v_1, v_2, \dots, v_k)$ represents is the concatenation of all those solutions associated with the edges therein, namely,

$$\tilde{\psi}_p := \bar{\psi}_{(v_1, v_2)} \bar{\psi}_{(v_2, v_3)} \cdots \bar{\psi}_{(v_{k-1}, v_k)} \quad (3)$$

where $\tilde{\psi}_p$ denotes the solution pair associated with the path p . For the notion of concatenation, see Definition 2.2.

HySST requires a library of possible inputs. The input library $(\mathcal{U}_C, \mathcal{U}_D)$ includes the input signals that can be

applied during flows (collected in \mathcal{U}_C) and the input values that can be applied at jumps (collected in \mathcal{U}_D).

HySST employs a pruning process to decrease the number of vertices in the search tree. This pruning operation is implemented by maintaining a *witness state set*, denoted as S , such that all the vertices within the vicinity of the witnesses are ignored except the one with lowest cost. For every witness s kept in S , a single vertex in the tree represents that witness. Such a vertex is stored in $s.rep$ for each witness $s \in S$.

HySST selects the vertex associated with the lowest cost within the vicinity of a randomly selected state. This vicinity of the randomly selected state, which we refer to as *random state neighborhood*, is defined by a ball of radius $\delta_{BN} \in \mathbb{R}_{>0}$. The pruning process removes from the search tree all the vertices within the vicinity of the closest witness to those removed vertices, which we refer to as *closest witness neighborhood* and is defined by a ball of radius $\delta_s \in \mathbb{R}_{>0}$. The pruning process does not remove the vertices in the closest witness neighborhood with lowest cost. Note that a vertex, say, v_a , may be associated to a higher cost than the costs associated with other vertices within the closest witness neighborhood of v_a , but has a child vertex, say, v_b , associated to the lowest cost compared with the costs of other vertices in the closest witness neighborhood of v_b . In this case, v_a should not be removed from the search tree because if it is removed, v_b is also removed due to being cascaded. However, even v_a is not removed, it will not be selected, and, therefore, will be kept in a separate set called inactive vertex set, denoted $V_{inactive}$. On the other hand, the vertices that are not pruned are stored in a set called the active vertex set, denoted V_{active} .

Next, we introduce the main steps executed by HySST. Given the optimal motion planning problem $\mathcal{P}^* = (X_0, X_f, X_u, (C, f, D, g), c)$ and the input library $(\mathcal{U}_C, \mathcal{U}_D)$, HySST performs the following steps:

- Step 1:** Sample a finite number of points from X_0 and initialize a search tree $\mathcal{T} = (V, E)$ by adding vertices associated with each sampling point and setting E as $E \leftarrow \emptyset$.
- Step 2:** Initialize the witness state set $S \subset \mathbb{R}^n$ by $S \leftarrow \emptyset$. For each $v \in V$ such that for all $v' \in V \setminus v$, $|\bar{x}_v - \bar{x}_{v'}| > \delta_s$, add the witness state $s = \bar{x}_v$ to S and set the representative of s as $s.rep \leftarrow v$. Initialize the active vertices set V_{active} by $V_{active} \leftarrow \{s.rep \in V : s \in S\}$. Initialize the inactive vertices set $V_{inactive}$ by $V_{inactive} \leftarrow \emptyset$.
- Step 3:** Randomly select one regime among flow regime and jump regime for the evolution of \mathcal{H} .
- Step 4:** Randomly select a point x_{rand} from C' (D') if the flow (jump, respectively) regime is selected in **Step 3**.
- Step 5:** Find all the vertices in V_{active} associated with the state values that are within δ_{BN} to x_{rand} and collect them in the set V_{BN} . Then, find the vertex in V_{BN} that has minimal cost, denoted v_{cur} . If no vertex is collected in V_{BN} , then find the vertex in

the search tree that has minimal distance to x_{rand} and assign it to v_{cur} .

Step 6: Randomly select an input signal (value) from \mathcal{U}_C (\mathcal{U}_D) if $\bar{x}_{v_{cur}} \in C' \setminus D'$ ($\bar{x}_{v_{cur}} \in D' \setminus C'$). Then, compute a solution pair denoted $\psi_{new} = (\phi_{new}, u_{new})$ starting from $\bar{x}_{v_{cur}}$ with the selected input applied via flow (jump, respectively). If $\bar{x}_{v_{cur}} \in D' \cap C'$, a random process is employed to decide to proceed the computation with flow or jump. Denote the final state of ϕ_{new} as x_{new} . Compute the cost at x_{new} , denoted c_{new} , by $c_{new} \leftarrow \bar{c}_{v_{cur}} + c(\phi_{new})$. If ψ_{new} does not intersect with X_u , then go to next step. Otherwise, go to **Step 3**.

Step 7: Find one of the witnesses in S that has minimal distance to x_{new} , denoted s_{near} , and proceed as follows:

- If $|s_{near} - x_{new}| > \delta_s$, then add a new witness $s_{new} = x_{new}$ to S and set its representative as x_{new} . Add a vertex v_{new} associated with x_{new} to V_{active} and an edge (v_{cur}, v_{new}) associated with ψ_{new} to E . Then, go to **Step 3**.
- If $|s_{near} - x_{new}| \leq \delta_s$,
 - if $\bar{c}_{s_{near}.rep} > c_{new}$, add a vertex v_{new} associated with x_{new} to V_{active} and an edge (v_{cur}, v_{new}) associated with ψ_{new} to E . Then, update the representative of s_{near} by the newly added vertex, i.e., $s_{near}.rep \leftarrow v_{new}$, and prune the vertex, say, v_{pre_near} which is previously witnessed by s_{near} . If v_{pre_near} is an inactive vertex, i.e., is such as v_a described above, then add v_{pre_near} to $V_{inactive}$. Otherwise, remove v_{pre_near} and all its child vertices from the search tree. Then, go to **Step 3**.
 - if $\bar{c}_{s_{near}.rep} \leq c_{new}$, go to **Step 3** directly.

B. HySST Algorithm

Following the overview above, the proposed algorithm is given in Algorithm 1. The inputs of Algorithm 1 are the problem $\mathcal{P}^* = (X_0, X_f, X_u, (C, f, D, g), c)$, the input library $(\mathcal{U}_C, \mathcal{U}_D)$, a parameter $p_n \in (0, 1)$, which tunes the probability of proceeding with the flow regime or the jump regime, an upper bound $K \in \mathbb{N}_{>0}$ for the number of iterations to execute, and two tunable sets $X_c \supset \bar{C}'$ and $X_d \supset D'$, which act as constraints in finding a closest vertex to x_{rand} . In addition, HySST requires additional parameters δ_{BN} and δ_s to tune the radius of random state neighborhood and closest witness neighborhood, respectively. Each function in Algorithm 1 is defined next.

1) $\mathcal{T}.init(X_0)$: The function call $\mathcal{T}.init$ is used to initialize a search tree $\mathcal{T} = (V, E)$. It randomly selects a finite number of points from X_0 . For each sampling point x_0 , a vertex v_0 associated with x_0 is added to V . At this step, no edge is added to E .

2) $return \leftarrow is_vertex_locally_the_best(x, cost, S, \delta_s)$: The function call $is_vertex_locally_the_best$ describes the

Algorithm 1 HySST algorithm

Input: $X_0, X_f, X_u, \mathcal{H} = (C, f, D, g), (\mathcal{U}_C, \mathcal{U}_D), p_n \in (0, 1), K \in \mathbb{N}_{>0}, X_c, X_d, \delta_{BN}$ and δ_s

- 1: $\mathcal{T}.init(X_0)$;
- 2: $V_{active} \leftarrow V, V_{inactive} \leftarrow \emptyset, S \leftarrow \emptyset$;
- 3: **for all** $v_0 \in V$ **do**
- 4: **if** $is_vertex_locally_the_best(\bar{x}_{v_0}, 0, S, \delta_s)$ **then**
- 5: $(S, V_{active}, V_{inactive}, E) \leftarrow$
 $prune_dominated_vertices(v_0, S, V_{active}, V_{inactive}, E)$
- 6: **end if**
- 7: **end for**
- 8: **for** $k = 1$ to K **do**
- 9: randomly select a real number r from $[0, 1]$;
- 10: **if** $r \leq p_n$ **then**
- 11: $x_{rand} \leftarrow random_state(\bar{C}')$;
- 12: $v_{cur} \leftarrow best_near_selection(x_{rand}, V_{active}, \delta_{BN}, X_c)$;
- 13: **else**
- 14: $x_{rand} \leftarrow random_state(D')$;
- 15: $v_{cur} \leftarrow best_near_selection(x_{rand}, V_{active}, \delta_{BN}, X_d)$;
- 16: **end if**
- 17: $(is_a_new_vertex_generated, x_{new}, \psi_{new}, cost_{new}) \leftarrow$
 $new_state(v_{cur}, (\mathcal{U}_C, \mathcal{U}_D), \mathcal{H}, X_u)$
- 18: **if** $is_a_new_vertex_generated$ &
 $is_vertex_locally_the_best(x_{new}, cost_{new}, S, \delta_s)$ **then**
- 19: $v_{new} \leftarrow V_{active}.add_vertex(x_{new}, cost_{new})$;
- 20: $E.add_edge(v_{cur}, v_{new}, \psi_{new})$;
- 21: $(S, V_{active}, V_{inactive}, E) \leftarrow$
 $prune_dominated_vertices(v_{new}, S, V_{active}, V_{inactive}, E)$;
- 22: **end if**
- 23: **end for**
- 24: **return** \mathcal{T} ;

conditions under which the state x is considered for addition to the search tree as is shown in Algorithm 2. First, Algorithm 2 looks for the closest witness s_{new} to x from the witness set S (line 1). If the closest witness is more than δ_s from x , then a new witness is added to S (lines 2 - 6). If s_{new} is just added as a witness or $cost$ is less than the cost of the closest witness's representative (line 7), then the state x with the cost $cost$ is locally optimal and a *true* signal is returned (line 8). Otherwise, a *false* signal is returned.

Algorithm 2 $is_vertex_locally_the_best(x, cost, S, \delta_s)$

- 1: $s_{new} \leftarrow nearest(S, x)$;
- 2: **if** $|x - s_{new}| > \delta_s$ **then**
- 3: $s_{new} \leftarrow x$
- 4: $s_{new}.rep \leftarrow NULL$
- 5: $S \leftarrow S \cup \{s_{new}\}$;
- 6: **end if**
- 7: **if** $s_{new}.rep == NULL$ or $cost < \bar{c}_{s_{new}.rep}$ **then**
- 8: **return true**;
- 9: **end if**
- 10: **return false**;

3) $(S, V_{active}, V_{inactive}, E) \leftarrow$
 $prune_dominated_vertices(v, S, V_{active}, V_{inactive}, E)$:

Algorithm 3 describes the pruning process of dominated vertices. First, Algorithm 3 looks for the witness s_{new} that is closest to \bar{x}_v and its representative v_{peer} (lines 1 - 2). The previous representative, which is dominated by v in terms of cost, is removed from the active set of vertices V_{active} and is added to the inactive vertices set $V_{inactive}$ (lines 4 - 5). Then, v replaces v_{peer} as the representative of s_{new} (line 7). If v_{peer} is a leaf vertex, then it can also safely be removed from the search tree (lines 8 - 13). The removal

of v_{peer} may cause a cascading effect for its parents, if they have already been in the inactive set $V_{inactive}$ and the only reason they were maintained in the search tree was because they were leading to v_{peer} . Here, the function call $isleaf(v_{peer})$ returns *true* signal if v_{peer} is a leaf vertex, which means v_{peer} does not have child vertices (line 8). The function call $parent(v_{peer})$ returns the parent vertex of v_{peer} (line 9).

Algorithm 3 $(S, V_{active}, V_{inactive}, E) \leftarrow$
 $prune_dominated_vertices(v, S, V_{active}, V_{inactive}, E)$

```

1:  $s_{new} \leftarrow nearest(S, \bar{x}_v)$ ;
2:  $v_{peer} \leftarrow s_{new}.rep$ ;
3: if  $v_{peer} \neq NULL$  then
4:    $V_{active} \leftarrow V_{active} \setminus \{v_{peer}\}$ ;
5:    $V_{inactive} \leftarrow V_{inactive} \cup \{v_{peer}\}$ ;
6: end if
7:  $s_{new}.rep \leftarrow v$ ;
8: while  $isleaf(v_{peer})$  and  $v_{peer} \in V_{inactive}$  do
9:    $v_{parent} \leftarrow parent(v_{peer})$ ;
10:   $E \leftarrow E \setminus \{(v_{parent}, v_{peer})\}$ ;
11:   $V_{inactive} \leftarrow V_{inactive} \setminus v_{peer}$ ;
12:   $v_{peer} \leftarrow v_{parent}$ ;
13: end while

```

4) $x_{rand} \leftarrow random_state(S)$: The function call $random_state$ randomly selects a point from the set $S \subset \mathbb{R}^n$. It is designed to select from $\overline{C'}$ and D' separately depending on the value of r rather than to select from $\overline{C'} \cup D'$. The reason is that if $\overline{C'}$ (D') has zero measure while D' ($\overline{C'}$) does not, the probability that the point selected from $\overline{C'} \cup D'$ lies in $\overline{C'}$ (D' , respectively) is zero, which would prevent finding a solution when one exists.

5) $v_{cur} \leftarrow best_near_selection(x_{rand}, V_{active}, \delta_{BN}, X_\star)$: The function call $best_near_selection$ searches for a vertex v_{cur} in the active vertex set V_{active} such that its associated state value is in the intersection between the set X_\star and $x_{rand} + \delta_{BN}\mathbb{B}$, and has minimal cost where \star is either c or d . This function is implemented by solving the following optimization problem.

Problem 3: Given $x_{rand} \in \mathbb{R}^n$, a radius $\delta_{BN} > 0$ of the random state neighborhood, a tunable state constraint set X_\star , and an active vertex set V_{active} , solve

$$\begin{aligned} \arg \min_{v \in V_{active}} \quad & \bar{c}_v \\ \text{s.t.} \quad & |\bar{x}_v - x_{rand}| \leq \delta_{BN} \\ & \bar{x}_v \in X_\star. \end{aligned}$$

The data of Problem 3 comes from the arguments of the $best_near_selection$ function call. This optimization problem can be solved by traversing all the vertices in V_{active} .

6) $(is_a_new_vertex_generated, x_{new}, \psi_{new}, cost_{new}) \leftarrow new_state(v_{cur}, (\mathcal{U}_C, \mathcal{U}_D), \mathcal{H}, X_u)$: If $\bar{x}_{v_{cur}} \in \overline{C'} \setminus D'$ ($\bar{x}_{v_{cur}} \in D' \setminus \overline{C'}$), the function call new_state generates a new solution pair ψ_{new} to hybrid system \mathcal{H} starting from $\bar{x}_{v_{cur}}$ by applying an input signal \tilde{u} (an input value u_D) randomly selected from \mathcal{U}_C (\mathcal{U}_D , respectively). If $\bar{x}_{v_{cur}} \in \overline{C'} \cap D'$, then this function generates ψ_{new} by randomly selecting flows or jump. The final state of $\psi_{new} = (\phi_{new}, u_{new})$ is denoted as x_{new} . The cost $cost_{new}$ at x_{new} is computed by $cost_{new} \leftarrow \bar{c}_{v_{cur}} + c(\phi_{new})$.

After ψ_{new} and x_{new} are generated, the function new_state checks if there exists $(t, j) \in \text{dom } \psi_{new}$ such that $\psi_{new}(t, j) \in X_u$. If so, then ψ_{new} intersects with the unsafe set and $is_a_new_vertex_generated \leftarrow false$. Otherwise, this function returns $is_a_new_vertex_generated \leftarrow true$.

7) $v_{new} \leftarrow V_{active}.add_vertex(x_{new}, cost_{new})$ and $E.add_edge(v_{cur}, v_{new}, \psi_{new})$: The function call $V_{active}.add_vertex(x_{new}, cost_{new})$ adds a new vertex v_{new} to V_{active} such that $\bar{x}_{v_{new}} \leftarrow x_{new}$ and $\bar{c}_{v_{new}} \leftarrow cost_{new}$ and returns v_{new} . The function call $E.add_edge(v_{cur}, v_{new}, \psi_{new})$ adds a new edge $e_{new} = (v_{cur}, v_{new})$ associated with ψ_{new} to E .

C. Solution Checking during HySST Construction

At each iteration, when a new vertex and a new edge are added to the search tree, i.e., $is_a_new_vertex_generated == true$, a solution checking function is employed to check if a path in \mathcal{T} can be used to construct a motion plan to the given motion planning problem. If this function finds a path $p = ((v_0, v_1), (v_1, v_2), \dots, (v_{n-1}, v_n)) =: (e_0, e_1, \dots, e_{n-1})$ in \mathcal{T} such that 1) $\bar{x}_{v_0} \in X_0$ and 2) $\bar{x}_{v_n} \in X_f$, then the solution pair $\tilde{\psi}_p$, defined in (3), is a motion plan to the given motion planning problem.

V. ASYMPTOTIC NEAR-OPTIMALITY ANALYSIS

This section analyzes the asymptotic optimality property of HySST algorithm. The following assumption assumes that the cost functional is Lipschitz continuous along the purely continuous solution pairs, locally bounded at jumps, and also satisfies additivity, monotonicity, and non-degeneracy.

Assumption 5.1: The cost functional $c : \Sigma_\phi \rightarrow \mathbb{R}_{\geq 0}$ satisfies the following:

- 1) It is Lipschitz continuous for all continuous solution pairs (ϕ_0, u_0) and (ϕ_1, u_1) such that $\phi_0(0, 0) = \phi_1(0, 0)$; specifically, there exists $K_c > 0$ such that $|c(\phi_0) - c(\phi_1)| \leq K_c \sup_{(t, 0) \in \text{dom } \phi_0 \cap \text{dom } \phi_1} \{|\phi_0(t, 0) - \phi_1(t, 0)|\}$.
- 2) For each purely discrete solution pairs (ϕ_0, u_0) and (ϕ_1, u_1) with one jump such that $\text{dom } \phi_0 = \text{dom } \phi_1 = \{0\} \times \{0, 1\}$ and $\phi_0(0, 0) = \phi_1(0, 0)$, there exists $K_d > 0$ such that $|c(\phi_0) - c(\phi_1)| \leq K_d \sup_{j \in \{0, 1\}} \{|\phi_0(0, j) - \phi_1(0, j)|\}$.
- 3) Consider two solution pair $\psi_0 = (\phi_0, u_0)$ and $\psi_1 = (\phi_1, u_1)$ such that their concatenation is $\psi_0 | \psi_1$. The following hold:
 - a) $c(\phi_0 | \phi_1) = c(\phi_0) + c(\phi_1)$ (additivity);
 - b) $c(\phi_1) \leq c(\phi_0 | \phi_1)$ (monotonicity);
 - c) For each $t_2 > t_1 \geq 0$ such that $(t_1, j) \in \text{dom } \psi_0$ and $(t_2, j) \in \text{dom } \psi_0$ for some $j \in \mathbb{N}$, there exists $M_c > 0$ such that $t_2 - t_1 \leq M_c |c(\phi_0(t_2, j)) - c(\phi_0(t_1, j))|$ (non-degeneracy during flows).
 - d) For each $j_1, j_2 \in \mathbb{N}$ such that $j_2 > j_1$, $(t, j_1) \in \text{dom } \psi_0$ and $(t, j_2) \in \text{dom } \psi_0$ for some $t \in \mathbb{R}_{\geq 0}$, there exists $M_d > 0$ such that $j_2 - j_1 \leq M_d |c(\phi_0(t, j_2)) - c(\psi_0(t, j_1))|$ (non-degeneracy at jumps).

Remark 5.2: Items 1) and 2) above guarantee that the cost of the nearby solution pairs are bounded by the distance between the solutions. Item 3) above guarantees that the cost of the solution pairs can be computed incrementally and that the global minimum of the cost functional can be found by the optimal motion planning problem.

Next we define the clearance of the potential motion plans, which is heavily used in the literature; see [16].

Definition 5.3 (Safety clearance of a solution pair):

Given a motion plan $\psi = (\phi, u)$ to the optimal motion planning problem $\mathcal{P}^* = (X_0, X_f, X_u, (C, f, D, g), c)$, the safety clearance δ_s of $\psi = (\phi, u)$ is equal to the maximal $\delta' > 0$ if the following hold:

- 1) $\phi(0, 0) + \delta'\mathbb{B} \subset X_0$;
- 2) For all $(t, j) \in \text{dom } \psi$, $(\phi(t, j) + \delta'\mathbb{B}, u(t, j) + \delta'\mathbb{B}) \cap X_u = \emptyset$.
- 3) $\phi(T, J) + \delta'\mathbb{B} \subset X_f$, where $(T, J) = \max \text{dom}(\phi, u)$.

Assumption 5.4: The optimal motion plan to the given optimal motion planning problem has positive safety clearance δ_s .

Definition 5.5 (Dynamics clearance of a solution pair):

Given a motion plan $\psi = (\phi, u)$ to the optimal motion planning problem $\mathcal{P}^* = (X_0, X_f, X_u, (C, f, D, g), c)$, the dynamics clearance δ_d of $\psi = (\phi, u)$ is equal to the maximal $\delta' > 0$ satisfying the following:

- 1) For all $(t, j) \in \text{dom } \psi$ such that I^j has nonempty interior, $(\phi(t, j) + \delta'\mathbb{B}, u(t, j) + \delta'\mathbb{B}) \subset C$;
- 2) For all $(t, j) \in \text{dom } \psi$ such that $(t, j + 1) \in \text{dom } \psi$, $(\phi(t, j) + \delta'\mathbb{B}, u(t, j) + \delta'\mathbb{B}) \subset D$.

Assuming that the optimal motion plan has positive dynamics clearance is restrictive for hybrid systems. Indeed, if the motion plan reaches the boundary of the flow set or of the jump set, then the motion plan has no clearance. To overcome this issue, the δ_f -inflation of hybrid systems, denoted $\mathcal{H}_{\delta_f} := (C_{\delta_f}, f_{\delta_f}, D_{\delta_f}, g_{\delta_f})$ for some $\delta_f > 0$, in our previous work is employed to create a positive dynamics clearance; see [10]. With both safety clearance and dynamics clearance defined, we are ready to define the clearance of the solution pair.

Definition 5.6 (Clearance of a solution pair): Given a motion plan $\psi = (\phi, u)$ to the optimal motion planning problem $\mathcal{P}^* = (X_0, X_f, X_u, (C, f, D, g), c)$, the clearance of $\psi = (\phi, u)$, denoted δ , is defined as the minimum of its safety clearance δ_s and dynamics clearance δ_d , i.e., $\delta := \min\{\delta_s, \delta_d\}$.

The following assumption relating the clearance δ of the optimal motion plan with the algorithm parameters δ_{BN} and δ_s is necessary to establish the optimality property.

Assumption 5.7: Given the clearance δ of the optimal motion plan, the parameters δ_{BN} and δ_s need to satisfy the following relationship

$$\delta_{BN} + 2\delta_s < \delta.$$

The following assumption is imposed on the input library.

Assumption 5.8: The input library $(\mathcal{U}_C, \mathcal{U}_D)$ is such that

- 1) Each input signal in \mathcal{U}_C is constant and \mathcal{U}_C includes all possible input signals such that their time domains are subsets of the interval $[0, T_m]$ for some $T_m > 0$ and their images belong to U_C . In other words, there exists $T_m > 0$ such that $\mathcal{U}_C = \{\tilde{u} : \text{dom } \tilde{u} = [0, T] \subset [0, T_m], \tilde{u} \text{ is constant and } \text{rge } \tilde{u} \in U_C\}$;
- 2) $\mathcal{U}_D = U_D$.

The following assumption is imposed on the random selection in HySST.

Assumption 5.9: The probability distributions of the random selection in the function calls *T.init*, *random_state*, and *new_state* are the uniform distribution.

The following assumptions are imposed on the flow map f and the jump map g of the hybrid system \mathcal{H} in (1).

Assumption 5.10: The flow map f is Lipschitz continuous. In particular, there exist $K_x^f, K_u^f \in \mathbb{R}_{>0}$ such that, for all (x_0, x_1, u_0, u_1) such that $(x_0, u_0) \in C$, $(x_0, u_1) \in C$, and $(x_1, u_0) \in C$,

$$\begin{aligned} |f(x_0, u_0) - f(x_1, u_0)| &\leq K_x^f |x_0 - x_1| \\ |f(x_0, u_0) - f(x_0, u_1)| &\leq K_u^f |u_0 - u_1|. \end{aligned}$$

Assumption 5.11: The jump map g is such that there exist $K_x^g \in \mathbb{R}_{>0}$ and $K_u^g \in \mathbb{R}_{>0}$ such that, for all $(x_0, u_0) \in D$ and $(x_1, u_1) \in D$,

$$|g(x_0, u_0) - g(x_1, u_1)| \leq K_x^g |x_0 - x_1| + K_u^g |u_0 - u_1|.$$

Then, we are ready to provide our main result showing that by feeding the the inflation of the original hybrid system, HySST would find a solution such that the cost is close to the minimal cost regardless of the positive dynamics clearance. See [12] for a detailed proof.

Theorem 5.12: Given an optimal motion planning problem $\mathcal{P}^* = (X_0, X_f, X_u, (C, f, D, g), c)$, suppose Assumptions 5.1, 5.7, 5.8, 5.9, 5.10, and 5.11 are satisfied and that there exists an optimal motion plan $\psi^* = (\phi^*, u^*)$ to \mathcal{P}^* satisfying Assumption 5.4 for some $\delta_s > 0$. When HySST is used to solve the motion planning problem $\mathcal{P}_{\delta_f}^* = (X_0, X_f, X_u, (C_{\delta_f}, f_{\delta_f}, D_{\delta_f}, g_{\delta_f}), c)$ where, for some $\delta_f > 0$, $(C_{\delta_f}, f_{\delta_f}, D_{\delta_f}, g_{\delta_f})$ denotes δ_f -inflation of (C, f, D, g) , the probability that HySST finds a motion plan $\psi = (\phi, u)$ such that $c(\phi) \leq (1 + \alpha\delta)c(\phi^*)$ converges to one as the number of iterations k goes to infinity for some constant $\alpha \geq 0$, where $\delta = \min\{\delta_s, \delta_f\}$.

VI. HYSST SOFTWARE TOOL FOR OPTIMAL MOTION PLANNING PROBLEMS FOR HYBRID SYSTEMS

Algorithm 1 leads to a software tool¹ to solve the optimal motion planning problems for hybrid systems. This software only requires the inputs listed in Algorithm 1. Next, HySST algorithm and this tool are illustrated in Examples 3.1 and 3.2.

Example 6.1: (Actuated bouncing ball system) The simulation result in Figure 2 shows that HySST is able to

¹Code at <https://github.com/HybridSystemsLab/hybridSST>.

find a motion plan for the instance of optimal motion planning problem for the actuated bouncing ball system. The

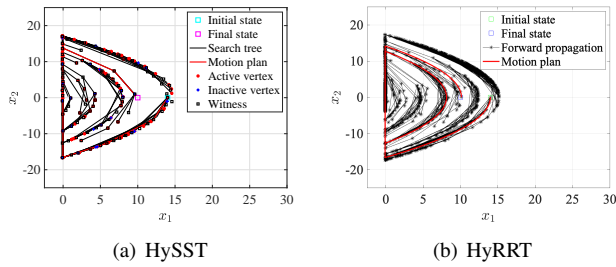


Fig. 2. Motion plans for actuated bouncing ball example solved by HySST and HyRRT in [10].

simulation is implemented in MATLAB and processed by a 3.5 GHz Intel Core i7 processor. Both HySST and HyRRT are run for 20 times to solve the same problem. The HySST creates 154 active vertices and 35 inactive vertices and takes 3.30 seconds, while HyRRT creates 660 vertices in total and takes 18.4 seconds on average. As is shown in Figure 2(a), only one jump occurs in the motion plans generated by HySST. Compared to the motion plans generated by HyRRT in Figure 2(b) where multiple jumps occur, the motion plan generated by HySST takes less hybrid time.

Example 6.2: (Collision-resilient tensegrity multicopter) The simulation result in Figure 3 shows that HySST is able to utilize the collision with the wall to decrease the hybrid time of the motion plan for multicopter. This simulation is computed on the same computation platform as the previous example, and the simulation for this problem takes 54.7 seconds and creates 2094 active vertices on average.

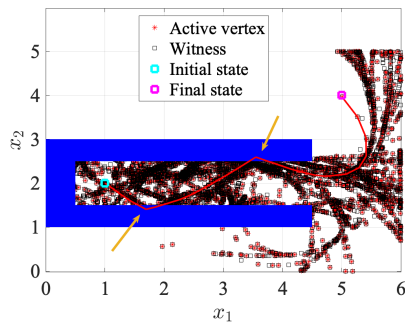


Fig. 3. The motion plan generated by HySST for collision-resilient tensegrity multicopter. The blue rectangles denote the obstacles that may cause the collision with the multicopter. The yellow arrows point to the location where collision occurs.

VII. CONCLUSION

In this paper, a HySST algorithm is proposed to solve optimal motion planning problems for hybrid systems. The proposed algorithm is illustrated in the bouncing ball and multicopter examples and the results show its capacity to solve the problem. In addition, this paper provides a result showing HySST algorithm is asymptotically near optimal under mild assumptions.

REFERENCES

- [1] S. M. LaValle, *Planning algorithms*. Cambridge university press, 2006.
- [2] G. T. Wilfong, “Motion planning for an autonomous vehicle,” in *Proceedings. 1988 IEEE International Conference on Robotics and Automation*. IEEE, 1988, pp. 529–533.
- [3] O. Khatib, “Real-time obstacle avoidance for manipulators and mobile robots,” in *Proceedings. 1985 IEEE international conference on robotics and automation*, vol. 2. IEEE, 1985, pp. 500–505.
- [4] L. E. Kavraki, P. Svestka, J.-C. Latombe, and M. H. Overmars, “Probabilistic roadmaps for path planning in high-dimensional configuration spaces,” *IEEE transactions on Robotics and Automation*, vol. 12, no. 4, pp. 566–580, 1996.
- [5] S. M. LaValle and J. J. Kuffner Jr, “Randomized kinodynamic planning,” *The international journal of robotics research*, vol. 20, no. 5, pp. 378–400, 2001.
- [6] Y. Yang, J. Pan, and W. Wan, “Survey of optimal motion planning,” *IET Cyber-Systems and Robotics*, vol. 1, no. 1, pp. 13–19, 2019.
- [7] O. Nechushtan, B. Raveh, and D. Halperin, “Sampling-diagram automata: A tool for analyzing path quality in tree planners,” in *WAFR*. Springer, 2010, pp. 285–301.
- [8] S. Karaman and E. Frazzoli, “Sampling-based algorithms for optimal motion planning,” *The international journal of robotics research*, vol. 30, no. 7, pp. 846–894, 2011.
- [9] Y. Li, Z. Littlefield, and K. E. Bekris, “Asymptotically optimal sampling-based kinodynamic planning,” *The International Journal of Robotics Research*, vol. 35, no. 5, pp. 528–564, 2016.
- [10] N. Wang and R. G. Sanfelice, “A rapidly-exploring random trees motion planning algorithm for hybrid dynamical systems,” in *2022 IEEE 61st Conference on Decision and Control (CDC)*. IEEE, 2022, pp. 2626–2631.
- [11] R. G. Sanfelice, *Hybrid feedback control*. Princeton University Press, 2021.
- [12] N. Wang and R. G. Sanfelice, “Hysst: A stable sparse rapidly-exploring random trees optimal motion planning algorithm for hybrid dynamical systems,” University of California, Santa Cruz, Department of Electrical and Computer Engineering, Tech. Rep., 2023, password: hysst23. [Online]. Available: <https://hybrid.soe.ucsc.edu/sites/default/files/preprints/TR-HSL-02-2023.pdf>
- [13] R. G. Sanfelice, “Hybrid feedback control,” 2021.
- [14] J. Zha and M. W. Mueller, “Exploiting collisions for sampling-based multicopter motion planning,” in *2021 IEEE International Conference on Robotics and Automation (ICRA)*. IEEE, 2021, pp. 7943–7949.
- [15] S. Liu, N. Atanasov, K. Mohta, and V. Kumar, “Search-based motion planning for quadrotors using linear quadratic minimum time control,” in *2017 IEEE/RSJ international conference on intelligent robots and systems (IROS)*. IEEE, 2017, pp. 2872–2879.
- [16] M. Kleinbort, K. Solovey, Z. Littlefield, K. E. Bekris, and D. Halperin, “Probabilistic completeness of rrt for geometric and kinodynamic planning with forward propagation,” *IEEE Robotics and Automation Letters*, vol. 4, no. 2, pp. x–xvi, 2018.